*Article*

# Thermodynamic Analysis of an Ethylene Reliquefaction System Using the Entropy-Cycle Method

**Viktoriia Sokolovska-Yefymenko [1], Larisa Morozyuk [1], Volodymyr Ierin [2],* and Oleksandr Yefymenko [1]**

[1]  Department of Cryogenic Technique, Odesa National University of Technology, 65039 Odessa, Ukraine
[2]  School of Mechatronics and Energy Engineering, NingboTech University, Ningbo 315100, China
*   Correspondence: yerinvladimir@gmail.com

**Abstract:** In this study, a boil-off gas reliquefaction system that is a part of liquid ethylene gas (LEG) carriers is evaluated. The reliquefaction system is formed by two thermally interconnected two-stage refrigeration cycles. The working fluid of the bottoming cycle is ethylene; the working fluid of the topping cycle is propylene. The research is based on determining the irreversibilities in the reliquefaction system cycles using the entropy-cycle method of thermodynamic analysis. The impact of the process performance in the main components on the reliquefaction system energy efficiency has been evaluated by the entropy-cycle method. The greatest thermodynamic irreversibility is observed in the two-stage compression process of the bottoming cycle (9%), total throttling irreversibility in the reliquefaction system (8.5%), and vapor superheating at the suction into the low stage of the two-stage compressor of the bottoming cycle (8%). The results of the study showed that it is necessary to improve the design of expansion devices using the replacement of throttle devices with ejectors when designing cascade ethylene reliquefaction plants. In addition, when operating such systems much attention should be paid to the condition of the insulation of cargo pipelines and the parameters of the cooling system of the cargo compressor.

**Keywords:** reliquefaction system; ethylene; thermodynamic analysis; entropy-cycle method; irreversibility

## 1. Introduction

Ethylene is one of the main products of the petrochemical industry. Liquefied ethylene's large sea transportations are carried out by specialized gas carriers (LEG carriers). Shipping by sea is a segment of the ethylene economy. The specialization of vessels is related to the cargo containment system and is determined by the physical properties of ethylene (normal boiling temperature is $-104\ °C$). A part of the transported ethylene (0.08–0.3% per day) evaporates, which leads to an increase in pressure and temperature in cargo tanks. To maintain constant pressure in the tanks, the boil-off gas (BOG) should be removed, condensated, and returned to the cargo tanks. A reliquefaction system is used for these purposes. The reliquefaction system is based on a low-temperature cascade refrigeration machine. The energy efficiency of vessel reliquefaction systems must comply with Energy Efficiency Design Index (EEDI) and Ship Energy Efficiency Management Plan (SEEMP) standards [1]. It is possible to increase the energy efficiency of the reliquefaction system by increasing productivity and reducing energy consumption.

There are studies dedicated to the LEG reliquefaction systems. Saputra and Supramono [2] evaluated an LPG vessel reliquefaction system with a capacity of 20 tons per day. The vessel carries both liquefied pressurized gases (propane and butane) and cryogenic liquids (ethylene, ethane, and methane). For the reliquefaction system, a cascade refrigeration machine is used. The thermodynamic analysis of the reliquefaction system has been conducted using the exergy analysis. Berlinck et al. [3] carried out a numerical simulation of the reliquefaction system.

Good agreement has been obtained between the assumed thermodynamic parameters and the experimental data. Chien and Shih [4] proposed a project for optimizing reliquefaction processes in the ethylene cargo containment systems. As a result of the exergy analysis, the operating conditions have been determined, in which the energy consumption is decreased by 16.2%. At the same time, the volumetric flow rates of refrigerant and boil-off gas are significantly reduced. The optimization of the real cycle for LEG by the exergy method was carried out by Li et al. [5]. The analysis showed an increase in the exergy efficiency of BOG liquefaction by 19% and a decrease in refrigerant flow rate by 45% per hour. Nanowski [6] described the ethylene cycle of a reliquefaction system using a Mollier diagram. The performance of a system with many refrigerants has been analyzed using experimental data. Tan et al. [7] proposed options for improving the energy efficiency of an ethylene reliquefaction system by using an ejector as an expansion device within a cascade refrigeration machine. The author of this study claims that the installation of an ejector reduces energy consumption by 15.7–27.9 kW compared to conventional expansion devices. In the studies of Tan et al. [8,9], three modified cycles of the ethylene reliquefaction system have been evaluated. The cycle parameters have been optimized to minimize the energy consumption of the entire system. The results showed that compressors and expansion devices observed the largest exergy losses. The authors provide background information on the selection of reliquefaction processes for LEG vessels.

Beladjine et al. presented a thermodynamic analysis of a cascade ethylene reliquefaction system [10]. This study considers various hydrocarbon refrigerants for application in the topping stage of the cascade. The conclusion is made about the expediency of using the refrigerant R600a. It is established that increasing the temperature of the tank leads to increasing the performance of the system. An overview of current maintenance programs and approaches to reducing the downtime of the main components of the reliquefaction plant has been carried out by Vorkapić et al. [11]. The importance of modern methods used in the practice of shipping is explained by the example of a modern reliquefaction system. The paper shows that ship companies adhere to conservative approaches (calendar maintenance), although modern systems require constant monitoring and prevention of equipment downtime. Wieczorek and Giernalczyk studied the problems encountered during loading and unloading operations when transporting ethylene by gas tankers [12]. The authors state that the most problematic operation in carrying out loading and unloading operations is the operation of gassing since it is associated with significant losses of ethylene. These losses lead in turn to large financial losses.

A literature review showed that very few works addressed the study of LEG liquefaction systems. The exergy analysis was intensively applied to evaluate the efficiency and optimize the thermodynamic cycle of the BOG reliquefaction system. The exergy method in the modern sense includes exergoeconomics; i.e., the analysis should include a lot of real cost indicators, which are very poorly suited to unification and make thermodynamic calculations time-consuming. It follows that the use of exergy analysis is appropriate for assessing the entire vessel energy system.

The purpose of the presented study is a thermodynamic analysis of the ethylene reliquefaction system cycle. To assess irreversible losses in the reliquefaction plant, in isolation from the power systems of the vessel, Morosuk et al. proposed using the entropy-cycle method of thermodynamic analysis [13]. The entropy-cycle method is a new direction in the development of graph-analytical methods for analyzing components of energy conversion systems [14–16]. Compared to exergy analysis; this method is less engineering. However, it provides information that can increase the creativity of the scientists to propose the option for the structural improvement of the reliquefaction system. In addition, the entropy-cycle method contains a visualization component for rapid assessment of the nature of the process. Both methods have the same theoretical basis, which is based on the Gouy–Stodola theorem, and show the same results.

## 2. LEG Reliquefaction System

For the numerical analysis, the data obtained for the vessel LEG reliquefaction system of the "ANTIKITIRA" tanker [17] have been used. This tanker belongs to the semi-refrigerated gas carriers. The tank design is an independent tank of type "C" [18]. To keep the pressure in the tank of the cargo close to the defined values, the vessel is equipped with a reliquefaction system. The flow diagram of the cascade direct reliquefaction system is shown in Figure 1. The reliquefaction system consists of two thermally interconnected two-stage refrigeration machines. The working fluids are ethylene (R1150) for the bottoming stage and propylene (R1270) for the topping stage.
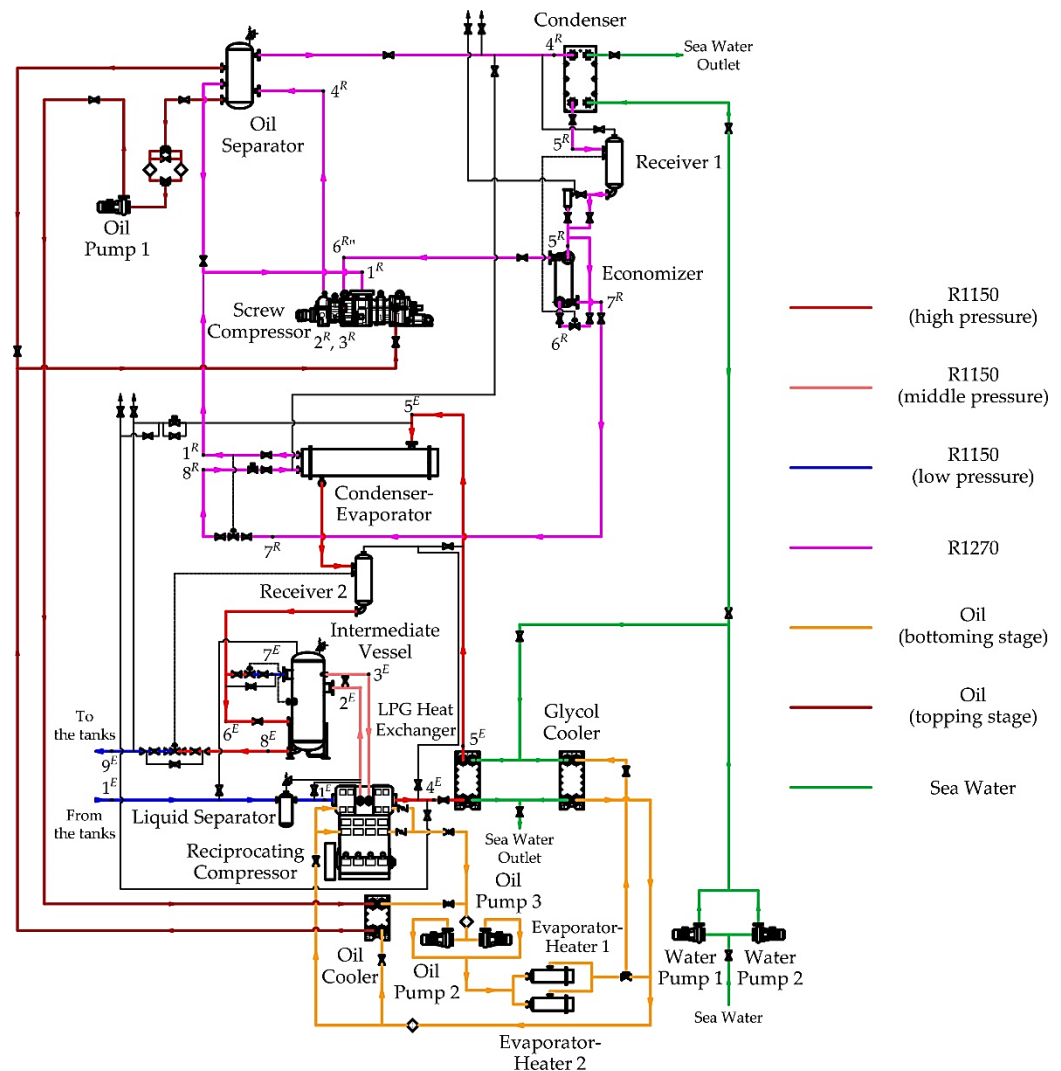


**Figure 1.** Flow diagram of the reliquefication system.

The bottoming stage of the cascade operates on a two-stage compression cycle with partial intercooling and parallel throttling. This refrigeration system includes a two-stage reciprocating crosshead compressor 2K140 by Burckhardt Compression [19], an intermediate vessel with a coil, an LPG condenser, a shell-and-tube condenser–evaporator, a receiver, shut-off, and control valves. The topping stage of the cascade operates on a two-stage compression cycle with incomplete intercooling and an economizer. This refrigeration system includes a two-stage oil-flooded screw compressor SS102944 by MYCOM [20] with a corresponding oil cooling system, a brazed-plate condenser, an economizer, shut-off, and control valves. Condenser–evaporator with intratubal evaporation of propylene is a common heat exchanger for both cascades.

The parameters and characteristics of the cycles obtained in real operating conditions when monitoring cargo operations were used for the thermodynamic analysis of the reliquefaction system (Figures 2 and 3). Based on these data, a thermodynamic cycle of the reliquefaction system (Figure 4) has been simulated (Table 1), and the mass flow rate definition and energy evaluation have been performed (Equations (1)–(7) and Table 2) [21].

ELETSON CORPORATION
COMPANY'S MANAGEMENT SYSTEM
PART V : FORMS & CHECKLISTS MANUAL (GAS)
SECTION 6 : CARGO & BUNKERING HANDLING
FCM-CBN027 - CARGO PLANT LOG SHEETS

ISSUE : 04 | REVISION : 00 | EFFECTIVE DATE : 05/04/18 | REVIEWED BY : WG | APPROVED BY : DP | PAGE : 1 OF 1

| Date/Time | Compressor | Mode | Capacity, % | Current Amr | 1ST STAGE Suc. T, °C | 1ST STAGE Suc. P, bar | 1ST STAGE Dis. T, °C | 1ST STAGE Dis P, bar | 2ST STAGE Suc. T, °C | 2ST STAGE Suc. P, bar | 2ST STAGE Dis. T, °C | 2ST STAGE Dis P, bar | Econ-ser Coil out. T, °C | Econ-ser lev.%, CCR | Econ-ser lev.cm, CCR | Condenser T, °C | Condenser P, bar | Condenser lev.%, CCR | Condenser lev.cm, CCR | Condenser SW P, bar | Condenser SW in T, °C | Condenser SW out T, °C | Lub oil Crankcase P, bar | Lub oil P, bar | Lub oil level, % | Lub oil Bulkhead seal T, °C | Lub oil Out cylinder T, °C | Lub oil Out crosshead T, °C | Glycol Pump disch. P, bar | Glycol Cooler in T, °C | Glycol Cooler out T, °C | Start | Stop | Total R/H |
|---|---|---|---|---|---|---|---|---|---|---|---|---|---|---|---|---|---|---|---|---|---|---|---|---|---|---|---|---|---|---|---|---|---|---|
| 17.08.2020 | P | 2 | 100 | 278 | -55.9 | 0.07 | 68 | 3.4 | 30.9 | 3.4 | 120 | 15.8 | -68.6 | 60 | 85 | 30 | 15.7 | 20 | 80 | 1 | 30.0 | 33.0 | | 0.50 | 4.5 | 50 | 39/40 | 37 | 39 | | | | | | |
| | C | 2 | 50 | 225 | -56.8 | 0.07 | 91 | 3.4 | 20.1 | 3.4 | 112 | 15.8 | | | | | | | | | | | | 0.50 | 4.5 | 50 | 39/41 | 38 | 39 | 4.6 | 45 | 37 | | | |
| | S | 2 | 100 | 265 | -56.8 | 0.08 | 72 | 3.5 | 14.5 | 3.5 | 107 | 15.8 | -70.5 | 60 | 85 | 30 | 15.7 | 20 | 80 | 1 | 30.0 | 33.0 | | 0.50 | 4.5 | 50 | 41/43 | 37 | 39 | | | | | | |
| 18.08.2020 | P | 2 | 100 | 278 | -58.3 | 0.18 | 66 | 4.0 | 27.2 | 4.0 | 117 | 17.5 | -66.1 | 60 | 85 | 30 | 17.4 | 20 | 80 | 1 | 30.0 | 33.0 | | 0.50 | 4.5 | 50 | 40/41 | 37 | 39 | | | | | | |
| | C | 2 | 50 | 225 | -57.7 | 0.18 | 92 | 4.0 | 13.1 | 4.0 | 111 | 17.5 | | | | | | | | | | | | 0.50 | 4.5 | 50 | 40/42 | 38 | 39 | 4.6 | 44 | 36 | | | |
| | S | 2 | 100 | 278 | -57.7 | 0.18 | 72 | 4.0 | 7.5 | 4.0 | 104 | 17.5 | -67.9 | 60 | 85 | 30 | 17.4 | 20 | 80 | 1 | 30.0 | 33.0 | | 0.50 | 4.5 | 50 | 42/43 | 38 | 39 | | | | | | |
| 19.08.2020 | P | 2 | 100 | 278 | -54.4 | 0.11 | 69 | 3.7 | 16.6 | 13.1 | 110 | 16.8 | -67.2 | 60 | 85 | 30 | 16.7 | 20 | 80 | 1 | 29.0 | 32.0 | | 0.50 | 4.5 | 50 | 39/41 | 37 | 39 | | | | | | |
| | C | 2 | 50 | 225 | -55.1 | 0.11 | 92 | 3.7 | 8.2 | 13.1 | 108 | 16.8 | | | | | | | | | | | | 0.50 | 4.5 | 50 | 39/41 | 38 | 39 | 4.6 | 44 | 36 | | | |
| | S | 2 | 100 | 252 | -55.1 | 0.11 | 74 | 3.7 | 9.4 | 3.7 | 106 | 16.8 | -69.2 | 60 | 85 | 30 | 16.7 | 20 | 80 | 1 | 29.0 | 32.0 | | 0.50 | 4.5 | 50 | 41/43 | 37 | 38 | | | | | | |
| 20.08.2020 | P | 2 | 100 | 278 | -53.2 | 0.04 | 71 | 3.4 | 18.6 | 3.4 | 113 | 15.6 | -68.8 | 60 | 85 | 30 | 15.5 | 20 | 80 | 1 | 29.0 | 32.0 | | 0.50 | 4.5 | 50 | 39/41 | 37 | 39 | | | | | | |
| | C | 2 | 50 | 212 | -54.3 | 0.03 | 92 | 3.4 | 15.1 | 3.4 | 111 | 15.5 | | | | | | | | | | | | 0.50 | 4.5 | 50 | 39/42 | 36 | 38 | 4.6 | 43 | 35 | | | |
| | S | 2 | 100 | 252 | -54.3 | 0.04 | 75 | 3.4 | 16.7 | 3.4 | 109 | 15.5 | -70.9 | 60 | 85 | 30 | 15.4 | 20 | 80 | 1 | 29.0 | 32.0 | | 0.50 | 4.5 | 50 | 41/43 | 36 | 38 | | | | | | |
| 21.08.2020 | P | | | | | | | | | | | | | | | | | | | | | | | | | | | | | | | | | 6:00 | |
| | C | | | | | | | | | | | | | | | | | | | | | | | | | | | | | | | | | 0:10 | |
| | S | | | | | | | | | | | | | | | | | | | | | | | | | | | | | | | | | 8:00 | |
| 22.08.2020 | P | | | | | | | | | | | | | | | | | | | | | | | | | | | | | | | | 4:00 | 8:00 | |
| | C | | | | | | | | | | | | | | | | | | | | | | | | | | | | | | | | 4:00 | 8:00 | |
| | S | | | | | | | | | | | | | | | | | | | | | | | | | | | | | | | | | | |
| 23.08.2020 | P | | | | | | | | | | | | | | | | | | | | | | | | | | | | | | | | | | 3344 |
| | C | | | | | | | | | | | | | | | | | | | | | | | | | | | | | | | | | | 3912 |
| | S | | | | | | | | | | | | | | | | | | | | | | | | | | | | | | | | | | 4486 |

**Figure 2.** Real-time monitoring of the cargo operation (cargo plant log sheet).

ELETSON CORPORATION
COMPANY'S MANAGEMENT SYSTEM
PART V : FORMS & CHECKLISTS MANUAL (GAS)
SECTION 6 : CARGO & BUNKERING HANDLING
FCM-CBN027 - REFRIGERATION PLANT LOG SHEETS (HMD8163~167.12K)

ISSUE : 04 | REVISION : 00 | EFFECTIVE DATE : 05/04/18 | REVIEWED BY : WG | APPROVED BY : DP | PAGE : 1 OF 1

**FCM-CBN027 - REFRIGERATION PLANT LOG SHEETS (HMD8163~167.12K)**

Cargo: Ethylene | Voyage: 13

| Date/Time | Time | Compressor | Compressor Load G3*51 (%) | Motor Current Amr | Suction T3*01 | Intermediate T3*42 | Discharge T3*62 | Receiver T3*12 | Eco Out T3*14 | Eth. Cond. Out T3*21 | Eth. Cond. Out T3*22 | Eth. Cond. Out T3*23 | Oil Separator T3*05 | Oil Supply T3*03 | Bulkhead | Water Outlet | Suction P3*01 | Discharge P3*04 | Receiver P3*11 | Oil Filter Diff. P3*15 | Oil Supply P3*17 | Receiver L3*01 | Oil Separator (T/M/B) | Start | Stop | Total R/H |
|---|---|---|---|---|---|---|---|---|---|---|---|---|---|---|---|---|---|---|---|---|---|---|---|---|---|---|
| 17.08.2020 | 12:00 | P | 98 | 342 | -35.2 | -16.1 | 74 | 37 | 36.4 | -37.8 | -38 | -37.5 | 43.4 | 46 | 53/60 | 38.0 | 0.10 | 3.6 | 15.0 | 0.1 | 18.0 | 32 | T | | | |
| | | S | 98 | 338 | -33.3 | -15.3 | 76 | 38 | 37.7 | -37.4 | -37 | -36.8 | 43.4 | 45 | 53/53 | 39.0 | 0.15 | 3.7 | 15.0 | 0.1 | 18.0 | 36 | T | | | |
| 18.08.2020 | 12:00 | P | 98 | 342 | -33.7 | -13.8 | 73 | 35 | 35 | -36.2 | -36 | -36.3 | 43.8 | 45 | 53/59 | 35.0 | 0.22 | 3.9 | 15.0 | 0.1 | 18.0 | 32 | T | | | |
| | | S | 98 | 338 | -32.8 | -14.9 | 75 | 36 | 35.9 | -36.7 | -36 | -35.8 | 43.6 | 45 | 54/54 | 36.0 | 0.21 | 3.8 | 15.0 | 0.1 | 18.0 | 36 | T | | | |
| 19.08.2020 | 12:00 | P | 98 | 338 | -35.1 | -15.1 | 74 | 35 | 35.1 | -37.1 | -37 | -36.8 | 43.9 | 45 | 53/59 | 37.0 | 0.16 | 3.7 | 15.0 | 0.1 | 18.0 | 32 | T | | | |
| | | S | 98 | 333 | -34.6 | -16.8 | 76 | 36 | 35.9 | -37.4 | -37 | -37.5 | 43.8 | 45 | 53/54 | 38.0 | 0.12 | 3.6 | 15.0 | 0.1 | 18.0 | 36 | T | | | |
| 20.08.2020 | 12:00 | P | 98 | 342 | -33.1 | -13.7 | 73 | 35 | 35.0 | -35.8 | -36 | -35.2 | 43.3 | 44 | 53/60 | 37.0 | 0.24 | 4.0 | 15.0 | 0.1 | 18.0 | 32 | T | | | |
| | | S | 98 | 342 | -31.7 | -13.8 | 75 | 36 | 35.9 | -35.3 | -37 | -36.6 | 43.2 | 44 | 53/55 | 38.0 | 0.21 | 3.9 | 15.0 | 0.1 | 18.0 | 35 | T | | | |
| 21.08.2020 | 12:00 | P | | | | | | | | | | | | | | | | | | | | | | T | | 6:00 | |
| | | S | | | | | | | | | | | | | | | | | | | | | | T | | 8:00 | |
| 22.08.2020 | 12:00 | P | | | | | | | | | | | | | | | | | | | | | | T | 4:00 | 8:00 | |
| | | S | | | | | | | | | | | | | | | | | | | | | | T | | | |
| 23.08.2020 | 12:00 | P | | | | | | | | | | | | | | | | | | | | | | T | | | 3974 |
| | | S | | | | | | | | | | | | | | | | | | | | | | T | | | 3979 |

**Figure 3.** Real-time monitoring of the cargo operations (refrigeration plant log sheet).

**Figure 4.** The thermodynamic cycle of the reliquefaction system in the *T–s* diagram.

**Table 1.** Initial data.

| Parameter | Value |
|---|---|
| The temperature of BOG (ethylene) in the tank $T_e$, °C | −38 |
| Condensing pressure in the condenser-evaporator $p^R_{c-e}$, bar | 16 |
| Intermediate pressure in cargo compressor $p^E_{int}$, bar | 4.45 |
| Intermediate pressure in screw compressor $p^R_{int}$, bar | 4.41 |
| Theoretical volumetric capacities of the cargo compressor low stage $V^{LS}_h$, m³·h⁻¹ | 609 * |
| Theoretical volumetric capacities of the cargo compressor high stage $V^{HS}_h$, m³·h⁻¹ | 273 * |

* Following the vessel's instructions.

**Table 2.** System simulation results.

| Parameter | Value |
|---|---|
| Refrigeration capacity $\dot{Q}_e$, kW | 92.5 |
| The mass flow rate of the refrigerant in the cargo low-stage compressor $\dot{m}^{LS}_e$, kg·s⁻¹ | 0.240 |
| The mass flow rate of the refrigerant in the coil $\dot{m}^R_e$, kg·s⁻¹ | 0.056 |
| The mass flow rate of the refrigerant in the cargo high-stage compressor $\dot{m}^{HS}_e$, kg·s⁻¹ | 3.550 |
| The mass flow rate of the refrigerant in the low-stage screw compressor $\dot{m}^{LS}_r$, kg·s⁻¹ | 0.400 |
| The mass flow rate of the refrigerant in the high-stage screw compressor $\dot{m}^{HS}_r$, kg·s⁻¹ | 0.562 |
| The mass flow rate of the refrigerant through the expansion valve in the topping stage of the cascade $\dot{m}^{EV}_r$, kg·s⁻¹ | 0.162 |
| Cargo compressor power consumption $\dot{W}^{CAR}_c$, kW | 115.17 |
| Screw compressor power consumption $\dot{W}^{SCR}_c$, kW | 80.92 |
| Total compressor power consumption $\sum \dot{W}_c$, kW | 196.09 |
| Coefficient of performance *COPact* | 0.47 |

The basic equations are written as follows.

The mass flow rate of the refrigerant in the cargo low-stage compressor is:

$$\dot{m}^{LS}_e = \frac{\dot{Q}_e}{h_{0E} - h_{9E}}. \tag{1}$$

The mass flow rate of the refrigerant in the coil is:

$$\dot{m}^R_e = \frac{\dot{m}^{LS}_e \cdot (h_{6E} - h_{8E})}{h_{7E''} - h_{7E'}}. \tag{2}$$

The mass flow rate of the refrigerant in the cargo high-stage compressor is:

$$\dot{m}_e^{HS} = \frac{\dot{m}_e^{LS} \cdot (1 - x_{7E}) + \dot{m}_e^R}{1 - x_{7E}}. \tag{3}$$

The mass flow rate of the refrigerant in the low-stage screw compressor is:

$$\dot{m}_r^{LS} = \frac{\dot{m}_e^{HS} \cdot (h_{5E} - h_{6E})}{h_{0R} - h_{8R}}. \tag{4}$$

The mass flow rate of the refrigerant through the expansion valve in the topping stage of the cascade is:

$$\dot{m}_r^{EV} = \frac{\dot{m}_r^{LS} \cdot (h_{5R} - h_{7R})}{h_{6R''} - h_{6R}}. \tag{5}$$

The mass flow rate of the refrigerant in the high-stage screw compressor is:

$$\dot{m}_r^{HS} = \dot{m}_r^{LS} + \dot{m}_r^{EV}. \tag{6}$$

The actual coefficient of performance (*COP*) is calculated by Equation (7):

$$COP_{act} = \frac{\dot{Q}_e}{\sum \dot{W}_c}. \tag{7}$$

## 3. Analysis by the Entropy-Cycle Method

The cycle of the presented cascade reliquefaction system with two-stage refrigeration machines in both stages of the cascades is a group of sequentially connected cycles. The cumulative effect of these cycles is equivalent to the effect of a single-stage cycle in the temperature range $T_c^E$ and $T_c^R$ [21]. The ideal cycle of such a cascade reliquefaction system can be represented based on a group of intersecting isotherms and adiabats in the *p-v* coordinate system (Figure 5): Carnot cycle 1, Carnot cycle 2, Carnot cycle 3, and Carnot cycle 4.
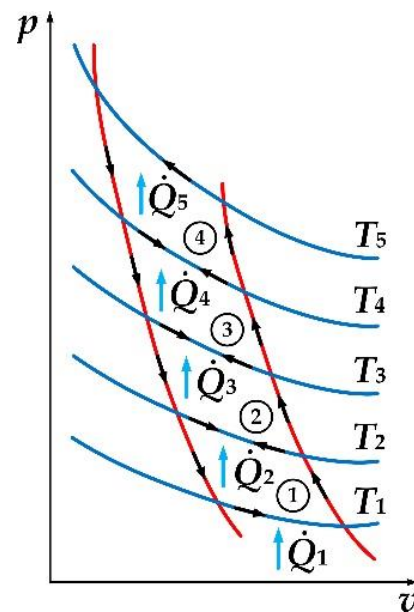


**Figure 5.** Carnot cycles in the *p-v* diagram.

The COP values can be written as:

$$\frac{1}{COP_{Car}} = 1 - \frac{T_4}{T_5} = 1 - \frac{\dot{Q}_4}{\dot{Q}_5}. \tag{8}$$

For all other cycles, Equation (7) can be conversed as follows:

$$\frac{T_4}{T_5} = \frac{\dot{Q}_4}{\dot{Q}_5}; \frac{T_3}{T_4} = \frac{\dot{Q}_3}{\dot{Q}_4}; \frac{T_2}{T_3} = \frac{\dot{Q}_2}{\dot{Q}_3}; \frac{T_1}{T_2} = \frac{\dot{Q}_1}{\dot{Q}_2}. \tag{9}$$

In Equation (9), the subscripts indicate the correspondence between the amount of heat that a particular source receives or rejects. At the same time, the sequence is preserved:

$$T_1 < T_2 < T_3 < T_4 < T_5. \tag{10}$$

After conversion Equation (10) can be written as:

$$T_5 : T_4 : T_3 : T_2 : T_1 = \dot{Q}_1 : \dot{Q}_2 : \dot{Q}_3 : \dot{Q}_4 : \dot{Q}_5 \Rightarrow \sum_{i=1}^{5} \frac{\dot{Q}_i}{T_i} = 0. \tag{11}$$

It follows from Equation (10) that for a sequential set of all four Carnot cycles, the cumulative effect is equivalent to the effect of the cycle operating in a range of temperatures $T_1$ and $T_5$. It should be noted that the reduced heat $\dot{Q}_i / T_i$ of any cycle does not take into account either the working fluid or its mass flow rate, but only the total amount of heat supplied and rejected is taken into account.

Based on the above, the use of the entropy-cycle method of thermodynamic analysis based on the well-known Gouy–Stodola (or so-called "lost work") theorem for analyzing the effectiveness of cascade multistage cycles is beyond doubt. Meanwhile, a detailed description of such an analysis is not given anywhere.

The entropy-cycle method consists in calculating a component-by-component analysis of changes (increment) in the entropy of all objects (internal and external) involved in the process of its functioning and calculating the total change in the entropy of the system as a whole [13,21]. When forming an actual cycle, it is customary to distinguish between two types of irreversibility: external irreversibility and internal irreversibility. This kind of irreversibility classification establishes the sources of energy irreversibilities in the system component and indicates ways to eliminate them.

The complexity of the analysis of the actual cycle is associated with the presence of specific working fluids in the stages of the cascade and the change in their mass flow rates. For thermodynamic analysis of the cascade refrigeration cycle, this cycle is divided into components: component 1 is the low mechanical compression stage of the bottoming stage of the cascade; component 2 is the high mechanical compression stage of the bottoming stage of the cascade; component 3 is the low mechanical compression stage of the topping stage of the cascade; component 4 is the high mechanical compression stage of the topping stage of cascade. All characteristics of the individual components are presented relative to 1 kg of the mass flow rate of the refrigerant of component 1 ($\dot{m}_e^{LS} = 1 \text{ kg·s}^{-1}$). Following the above, the relative mass flow rates of working fluids in the stages of the cascade can be represented as follows.

The relative mass flow rate of the refrigerant in the cargo high-stage compressor is:

$$g_1 = \frac{\dot{m}_e^{HS}}{\dot{m}_e^{LS}}. \tag{12}$$

The relative mass flow rate of the refrigerant in the low-stage screw compressor is:

$$g_2 = \frac{\dot{m}_r^{LS}}{\dot{m}_e^{HS}}. \tag{13}$$

The relative mass flow rate of the refrigerant in the high-stage screw compressor is:

$$g_3 = \frac{\dot{m}_r^{HS}}{\dot{m}_r^{LS}}. \tag{14}$$

The coefficient of performance of the cycle with adiabatic processes is calculated by Equation (15):

$$COP_a = \frac{h_{0E} - h_{9E}}{(h_{4R} - h_{5R}) \cdot g_1 \cdot g_2 \cdot g_3 - (h_{0E} - h_{9E})}. \tag{15}$$

The analysis is carried out at an initially assumed constant temperature: evaporating temperature $T_e$, ambient temperature $T_{amb}$, the condensing temperature in the bottoming stage $T_c^E$, the condensing temperature in the topping stage $T_c^R$, the temperature in the condenser-evaporator $T_{c-e}$, and temperature difference in the heat exchangers of the components $\Delta T$. The corresponding Carnot cycle can be used as a cycle model for the studied components with the processes of heat supply and rejection during phase transformations of single-component fluids (Figure 6).
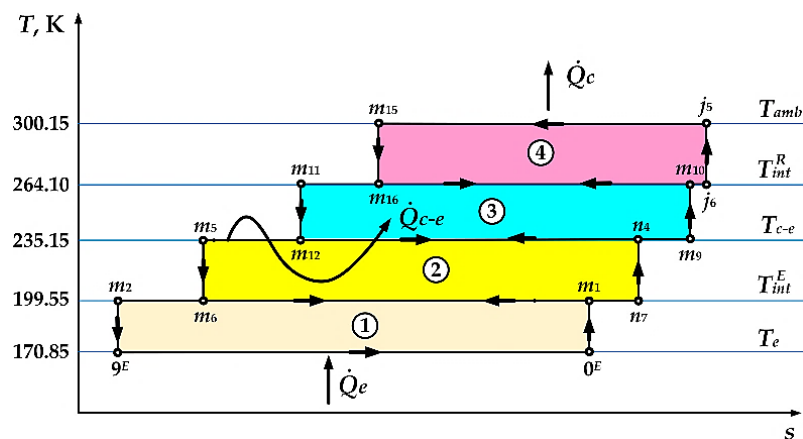


**Figure 6.** Cycle model of the cascade refrigeration system in the *T–s* diagram.

The temperature range of the Carnot cycle for component 1 is from $T_e$ to $T_{int}^E$, for component 2 is from $T_{int}^E$ to $T_{c-e}$, for component 3 is from $T_{c-e}$ to $T_{int}^R$, and for component 4 is from $T_{int}^R$ to $T_{amb}$. According to the working fluids, the cycle models are presented as Carnot 1 and Carnot 2 for bottoming stage of the cascade as well as Carnot 3 and Carnot 4 for the topping stage of the cascade. The areas of the corresponding Carnot cycles are equivalent to the works of the cycles. Based on the theoretical studies of Morosuk et al., [13] should be calculated starting from component 2, taking into account the changed mass flow rates of working fluids in the stages. In a graphic representation, this corresponds to an increase in the area along the *x*-axis (entropy *s*).

The analysis has been carried out graphically way using the *T–s* diagram (Figures 7 and 8). The cycles are compared by step-by-step replacement of growing total irreversibilities by changing the width of the corresponding Carnot cycle. The actual cycle of the bottoming stage of the cascade is represented by the contour $0^E1^E2^E3^E4^E5^E6^E7^E8^E9^E$ (Figure 7). The image of the cycles takes into account external irreversibility in the processes of heat rejection and supply as well as internal irreversibility of the compression processes in LS(E) and HS(E) compressors and throttling in EV1(E) and EV2(E) in expansion valves. The

corresponding Carnot cycle 1 is constructed with the equality of useful effects of the Carnot cycle, and the actual cycle is:

$$Area\ d0^E9^Eb \rightarrow q_e = h_{0E} - h_{9E} = T_{amb} \cdot (s_{0E} - s_{9E}). \tag{16}$$
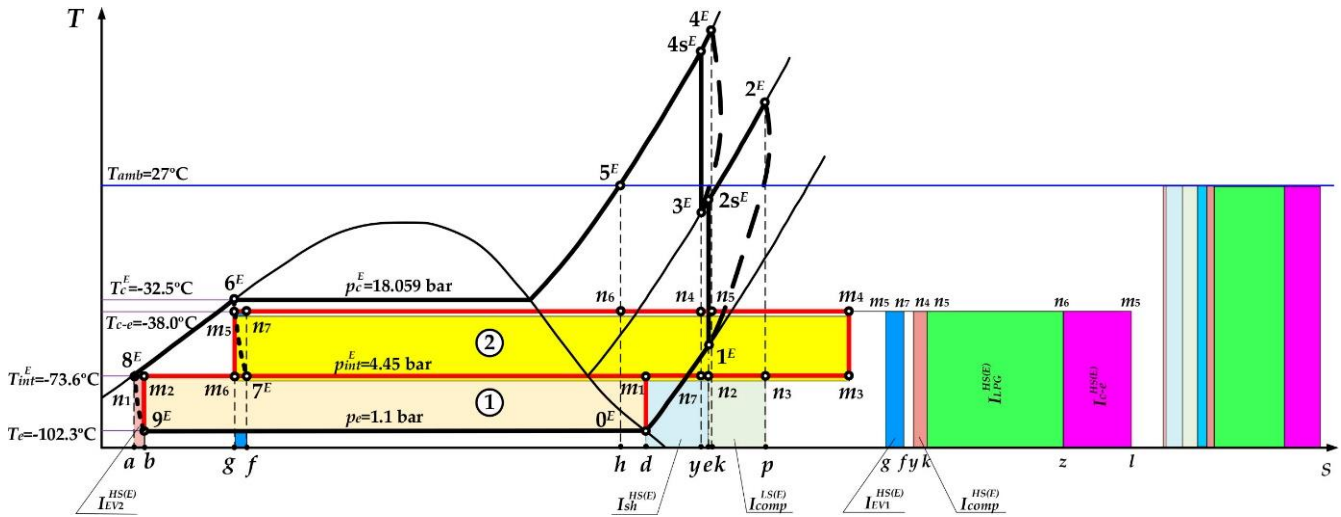


**Figure 7.** Determination of irreversibilities in the bottoming stage of the cascade ethylene reliquefaction system.
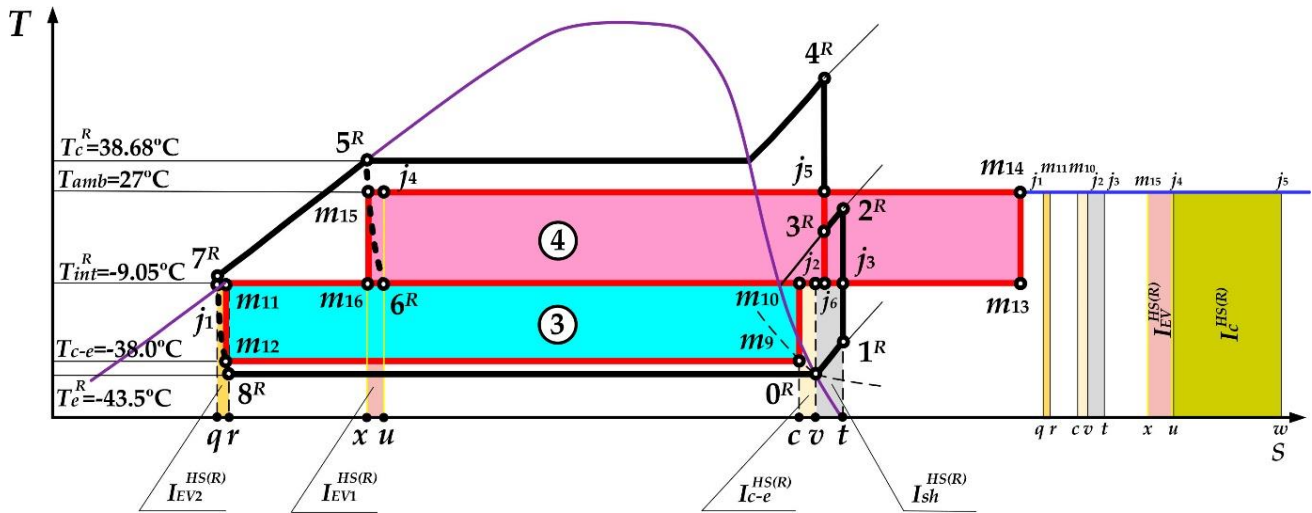


**Figure 8.** Determination of irreversibilities in the topping stage of the cascade ethylene reliquefaction system.

The Carnot cycle1 is represented by the area $0^Em_1m_29^E$. To construct the corresponding Carnot cycle 2, it is used the ratio of mass flow rates for the high and low stages of the bottoming stage of the cascade $g_1$ (Equation (12)).

Carnot cycle 2 is built on the temperatures $T_c^E$ and $T_{c-e}$ between the stages and represented by the area $n_7n_4m_5m_6$. Considering the change in the flow rate of the working fluid $g$, Carnot cycle 2 along the *x*-axis (entropy *s*) is increased on the right—area $m_3m_4m_5m_6$.

The calculation model on the example of the bottoming stage of the cascade refrigeration cycle is represented by Equations (17)–(29). The geometric interpretation of the parameters obtained in these equations is represented by figures having the appropriate area and described by letters in Figure 7.

The specific work of compression in the LS(E) compressor of the actual cycle is:

$$w^{LS(E)} = h_{2^E} - h_{1^E}. \tag{17}$$

The specific work in the corresponding Carnot cycle 1 is:

$$w_{Car}^{LS(E)} = (h_{m_1} - h_{0^E}) - (h_{m_2} - h_{9^E}) \Leftrightarrow Area \; 0^E m_1 m_2 9^E. \tag{18}$$

The difference of specific works from Equations (17) and (18) is:

$$w_{cycle}^{LS(E)} = w^{LS(E)} - w_{Car}^{LS(E)}. \tag{19}$$

The irreversibility in the LS(E) compressor is:

$$I_{comp}^{LS(E)} = T_c^E \cdot (s_p - s_e) = T_{amb} \cdot \Delta s_{comp}^{LS(E)} \Leftrightarrow Area \; p n_3 n_2 e. \tag{20}$$

The irreversibility due to vapor superheating inlet the LS(E) compressor is:

$$I_{sh}^{LS(E)} = T_c^E \cdot (s_e - s_d) = T_{amb} \cdot \Delta s_{sh}^{LS(E)} \Leftrightarrow Area \; e n_2 m_1 d. \tag{21}$$

The irreversibility in the expansion valve EV2(E) is:

$$I_{EV2}^{LS(E)} = T_c^E \cdot (s_b - s_a) = T_{amb} \cdot \Delta s_{EV2}^{LS(E)} \Leftrightarrow Area \; a b 9^E m_2 n_1. \tag{22}$$

The specific work of compression in the HS(E) compressor of the actual cycle is:

$$w^{HS(E)} = (h_{4^E} - h_{3^E}) \cdot g. \tag{23}$$

The specific work in the corresponding Carnot cycle 2 is:

$$W_{Car}^{HS(E)} = [(h_{n_4} - h_{n_7}) - (h_{m_5} - h_{m_6})] \cdot g \Leftrightarrow Area \; m_3 m_4 m_5 m_6. \tag{24}$$

The difference of specific works from Equations (23) and (24) is:

$$w_{cycle}^{HS(E)} = w^{HS(E)} - w_{Car}^{HS(E)}. \tag{25}$$

The irreversibility in the HS(E) compressor is:

$$I_{comp}^{HS(E)} = \left[ T_{cc} \cdot (s_k - s_y) \right] \cdot g = T_{amb} \cdot \Delta s_{comp}^{HS(E)} \Leftrightarrow Area \; k n_5 n_4 y g. \tag{26}$$

The irreversibility in the expansion valve EV1(E) is:

$$I_{EV1}^{HS(E)} = \left[ T_{c-e} \cdot \left( s_f - s_g \right) \right] \cdot g = T_{amb} \cdot \Delta s_{EV1}^{HS(E)} \Leftrightarrow Area \; m_4 n_7 g f. \tag{27}$$

The irreversibility in the LPG heat exchanger (see Figure 1) is:

$$I_{LPG}^{HS(E)} = [(h_{4^E} - h_{5^E}) - T_{c-e} \cdot (s_k - s_h)] \cdot g = T_{amb} \cdot \Delta s_{LPG}^{HS(E)} \Leftrightarrow Area \; k n_5 n_6 h. \tag{28}$$

The irreversibility in the condenser-evaporator is:

$$I_{c-e}^{HS(E)} = \left[ (h_{5^E} - h_{6^E}) - T_{c-e} \cdot \left( s_k - s_g \right) \right] \cdot g = T_{amb} \cdot \Delta s_{c-e}^{HS(E)} \Leftrightarrow Area \; g m_5 n_6 h. \tag{29}$$

The results of calculations of irreversibilities in individual processes of the bottoming stage of the cascade are presented in Table 3. When calculating the system's parameters, the database REFPROP 10.0 software has been used to determine the properties of working fluids [22].

**Table 3.** The analysis of the bottoming stage of the cascade system.

| Parameter | Value |
|---|---|
| The difference between specific works from Equations (3) and (4) $w_{cycle}^{LS(E)}$, kJ·kg$^{-1}$ | 118.52 |
| The irreversibility in the LS(E) compressor $I_{comp}^{LS(E)}$, kJ·kg$^{-1}$ | 52.42 |
| The irreversibility due to vapor superheating inlet the LS(E) compressor $I_{sh}^{LS(E)}$, kJ·kg$^{-1}$ | 61.47 |
| The irreversibility in the expansion valve EV2(E) $I_{EV2}^{LS(E)}$, kJ·kg$^{-1}$ | 65.92 |
| The difference between specific works from Equations (9) and (10), $w_{cycle}^{HS(E)}$ kJ·kg$^{-1}$ | 17.04 |
| The irreversibility in the HS(E) compressor $I_{comp}^{HS(E)}$, kJ·kg$^{-1}$ | 34.35 |
| The irreversibility in the expansion valve EV1(E) $I_{EV1}^{HS(E)}$, kJ·kg$^{-1}$ | 19.21 |
| The irreversibility in the LPG heat exchanger $I_{LPG}^{HS(E)}$, kJ·kg$^{-1}$ | 10.97 |
| The irreversibility in the condenser-evaporator $I_{c-e}^{HS(E)}$, kJ·kg$^{-1}$ | 32.34 |

Note: The specific values of kJ kg$^{-1}$ are related to 1 kg of cargo (ethylene).

Analysis of the topping stage of cascade and graphical interpretation of the corresponding cycles Carnot 3 and Carnot 4 is carried out similarly to the above but with the condition of the influence of the working fluids flow rate over the stages of the topping cycle of the cascade $g_2$ and $g_2$ (Equations (13) and (14)). The actual cycle is represented by the contour $0^R1^R2^R3^R4^R5^R6^R7^R8^R$ (Figure 8). The results of calculations of irreversibilities in individual processes of the topping stage of the cascade are presented in Table 4.

**Table 4.** The analysis of the topping stage of the cascade system.

| Parameter | Value |
|---|---|
| The difference between specific works $w_{cycle}^{LS(R)}$, kJ·kg$^{-1}$ | 34.31 |
| The irreversibility in the expansion valve EV2(R) $I_{EV2}^{LS(R)}$, kJ·kg$^{-1}$ | 10.81 |
| The irreversibility due to vapor superheating inlet of the LS(R) compressor $I_{sh}^{LS(R)}$, kJ·kg$^{-1}$ | 27.06 |
| The difference between specific works $w_{cycle}^{HS(R)}$, kJ·kg$^{-1}$ | 65.58 |
| The irreversibility in the expansion valve EV1(R) $I_{EV1}^{HS(R)}$, kJ·kg$^{-1}$ | 30.88 |
| The irreversibility in the condenser-evaporator $I_{c-e}^{HS(R)}$, kJ·kg$^{-1}$ | 18.16 |
| The irreversibility in the condenser $I_c^{HS(R)}$, kJ·kg$^{-1}$ | 43.60 |

Note: The specific values of kJ kg$^{-1}$ are related to 1 kg of refrigerant (propylene).

The effectiveness of a thermodynamic cycle is:

$$\eta = \frac{COP_a}{COP_{Car}},\tag{30}$$

where $COP_{Car}$ is the coefficient of performance of the Carnot cycle:

$$COP_{Car} = \frac{T_e}{T_{amb} - T_e}.\tag{31}$$

Provided that the beneficial effects are equal in the actual cycle (Figure 4) and the Carnot cycle, the effectiveness can be defined as:

$$\eta = \frac{w_{Car,TOT}}{w_{TOT}},\tag{32}$$

where $w_{Car,\,TOT}$ and $w_{TOT}$ are the total specific work of the corresponding Carnot cycles and actual cycle for the cascade refrigeration system, respectively:

$$w_{Car,TOT} = w_{Car}^{LS(E)} + w_{Car}^{HS(E)} + w_{Car}^{LS(R)} + w_{Car}^{HS(R)},\tag{33}$$

$$w_{TOT} = w^{LS(E)} + w^{HS(E)} + w^{LS(R)} + w^{HS(R)}.\tag{34}$$

A graphical interpretation of the results of the thermodynamic performance assessment according to calculations is shown in Figure 9. Here, 57% is associated with the specific work of the corresponding Carnot cycles for the cascade refrigeration machine. The analysis shows that in the evaluated actual cycle of the cascade refrigeration machine, the greatest impact on energy efficiency (i.e., decreasing the irreversibility) is associated with the two-stage compressor of the bottoming stage of the cascade $I_{comp}^{E}$ (9%), expansion devices $I_{EV.TOT}$ (8.5%), and the process of superheating of the vapor at the suction in a cargo compressor $I_{sh}^{LS(R)}$ (8%).
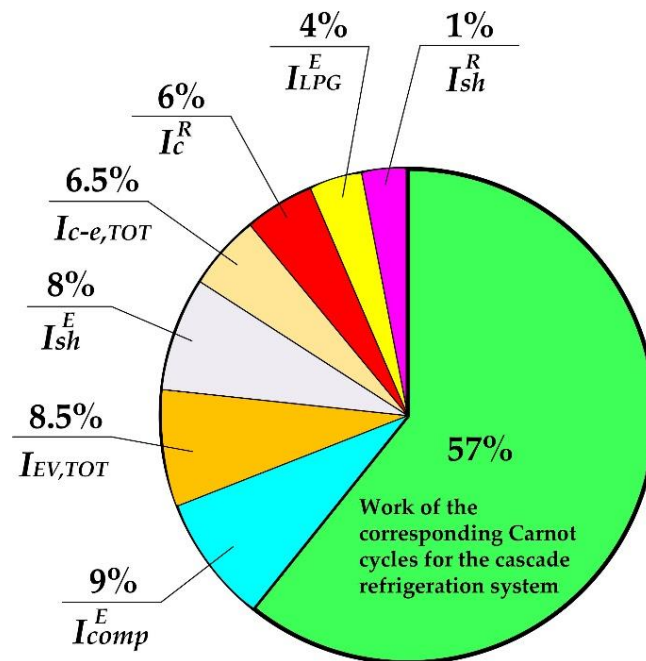


**Figure 9.** A graphical interpretation of the results of the thermodynamic performance assessment.

As follows from the results obtained, when designing cascade ethylene reliquefaction systems, first of all, it is necessary to focus on reducing irreversibility in the cargo compressor by diagnosing the cooling system and ensuring its efficient operation. The current irreversibility value in the cargo compressor seems to be related to improper operation of the refrigeration system on a particular vessel. A noticeable increase in efficiency can be obtained by reducing irreversibility in expansion devices (because the expansion device cannot be improved itself). In particular, Tan et al. propose to use of ejectors as expansion devices, which leads to an increase in the COP of the system by 5.3% [7]. In addition, when designing cascade ethylene reliquefaction systems, much attention should be paid to the insulating design of cargo pipelines.

## 4. Conclusions

In this study, the entropy-cycle method of thermodynamic analysis has been applied to assess the energy efficiency of complex multi-stage cascade refrigeration cycles, since this method has great visual possibilities and associated creativity to develop the options for structurally improving the systems.

Based on the results of the analysis obtained by the entropy-cycle method, the impact of all the main components on the energy efficiency of the ethylene reliquefaction system was evaluated. The following processes have the highest thermodynamic irreversibility: compression in a two-stage compressor of the bottoming stage $I_{comp}^{E}$ (9%), the total process of throttling in the reliquefaction system $I_{EV.TOT}$ (8.5%), and the process of superheating of the vapor at the suction in a cargo compressor $I_{sh}^{LS(R)}$ (8%).

Thus, when designing cascade ethylene reliquefaction systems, first of all, much attention should be paid to reducing irreversibility in the cargo compressor by diagnosing the cooling system and ensuring its efficient operation, using ejectors as expansion devices, and improving the insulating design of cargo pipelines.

## Nomenclature

| | |
|---|---|
| $g$ | relative mass flow rates |
| $h$ | specific enthalpy, $kJ \cdot kg^{-1}$ |
| $I$ | irreversibility, $kJ \cdot kg^{-1}$ |
| $\dot{m}$ | mass flow rate, $kg \cdot s^{-1}$ |
| $p$ | pressure, bar |
| $\dot{Q}_e$ | refrigeration capacity, kW |
| $s$ | specific entropy, $kJ \cdot kg^{-1} \cdot K$ |
| $T$ | temperature, °C |
| $V_h$ | theoretical volumetric capacities of the compressor, $m^3 \cdot h^{-1}$ |
| $w$ | specific work, $kJ \cdot kg^{-1}$ |
| $\dot{W}_c$ | compressor power consumption, kW |
| $x$ | liquid quality, $kg \cdot kg^{-1}$ |
| $COP$ | coefficient of performance |
| Acronyms | |
| BOG | boil-off gas |
| EEDI | Energy efficiency design index |
| LEG | liquefied ethylene gas |
| LPG | liquefied petroleum gas |
| SEEMP | Ship energy efficiency management plan |
| Greek symbols | |
| Δ | difference |
| Subscripts | |
| $c$ | condenser |
| $Car$ | Carnot |
| $c\text{-}e$ | condenser-evaporator |
| $e$ | evaporator |
| $EV$ | expansion valve |
| $int$ | intermediate |
| $r$ | refrigerant |
| $TOT$ | total |
| $1, 2 \ldots 9$ | state of cycle |

Superscripts

| | |
|---|---|
| ′ | saturated liquid |
| ″ | saturated vapor |
| *CAR* | cargo compressor |
| *E* | ethylene |
| *HS* | high stage |
| *LS* | low stage |
| *RH* | high boiling component |
| *R* | refrigerant |
| *SCR* | screw compressor |
| *RL* | low boiling component |

## References

1. Annex VI of MARPOL 73/78-Regulations for the Prevention of Air Pollution from Ships. Available online: https://www.maritimenz.govt.nz/rules/MARPOL-Annex-VI/default.asp (accessed on 20 August 2022).
2. Saputra, S.; Supramono, D. Optimization of Propane Reliquefaction Cycle in LPG Plant. In Proceedings of the 2019 IEEE International Conference on Innovative Research and Development (ICIRD), Jakarta, Indonesia, 28–30 June 2019; pp. 1–6.
3. Berlinck, E.C.; Parise, J.A.R.; Pitanga Marques, R. Numerical simulation of an ethylene reliquefaction plant. *Int. J. Energy Res.* **1997**, *21*, 597–614. [CrossRef]
4. Chien, M.H.; Shih, M.Y. An Innovative Optimization Design for a Boil-off Gas Reliquefaction Process of LEG Vessels. *J. Pet.* **2011**, *47*, 65–74.
5. Li, Y.; Jin, G.; Zhong, Z. Thermodynamic Analysis-Based Improvement for the Boil-off Gas Reliquefaction Process of Liquefied Ethylene Vessels. *Chem. Eng. Technol.* **2012**, *35*, 1759–1764. [CrossRef]
6. Nanowski, D. The Influence of Incondensable Gases on the Refrigeration Capacity of The Reliquefaction Plant during Ethylene Carriage by Sea. *J. KONES Powertrain Transp.* **2016**, *3*, 359–364. [CrossRef]
7. Tan, H.; Sun, N.; Zhao, Q.; Li, Y. An ejector-enhanced reliquefaction process (EERP) for liquid ethylene vessels. *Int. J. Energy Res.* **2017**, *41*, 658–672. [CrossRef]
8. Tan, H.; Cai, W.; Wang, Q.-G.; Sun, N. Optimization and comparison of boiling-off gas reliquefaction processes for liquid ethylene vessels. In Proceedings of the 2016 IEEE 11th Conference on Industrial Electronics and Applications (ICIEA), Hefei, China, 5–7 June 2016; pp. 717–722. [CrossRef]
9. Tan, H.; Zhang, Y.; Shan, S.; Zhao, Q. Comparative study of boil-off gas reliquefaction processes for liquid ethylene vessels. *J. Mar. Sci. Technol.* **2019**, *24*, 209–220. [CrossRef]
10. Beladjine, B.M.; Ouadha, A.; Addad, Y. Thermodynamic analysis of hydrocarbon refrigerants-based ethylene BOG re-liquefaction system. *J. Mar. Sci. Appl.* **2016**, *15*, 321–330. [CrossRef]
11. Vorkapić, A.; Kralj, P.; Martinović, D. The analysis of the maintenance systems of a LPG carrier's liquefaction system main components. *Sci. J. Marit. Res.* **2017**, *31*, 3–9. [CrossRef]
12. Wieczorek, A.; Giernalczyk, M. Operational Problems of Ethylene Transport by LPG Gas Carriers. *J. KONES* **2019**, *26*, 191–197. [CrossRef]
13. Morosuk, T.; Nikulshin, R.; Morosuk, L. Entropy-cycle method for analysis of refrigeration machine and heat pump cycles. *Therm. Sci.* **2006**, *10*, 111–124. [CrossRef]
14. Morosuk, T.; Tsatsaronis, G. A new approach to the exergy analysis of absorption refrigeration machines. *Energy* **2008**, *33*, 890–907. [CrossRef]
15. Bobilov, V.; Iliev, I.; Zlatev, P.; Kolev, Z.; Genchev, G.; Mushakov, P. Graph-analytical method for estimation of flows' distribution in low-pressure gas transport systems. In Proceedings of the 2nd International Conference of Thermal Equipment, Renewable Energy and Rural Development (TE-RE-RD 2013), Băile Olăneşti, Romania, 20–22 July 2013; pp. 9–14.
16. İbrahİmoğlu, B. Determination of 1/V-T (P, constant) diagrams of hydrogen gases by graph-analytical methods. *J. Therm. Eng.* **2017**, *3*, 1071–1077. [CrossRef]
17. VesselFinder. ANTIKITHIRA, LPG Tanker, IMO 9788980. 2021. Available online: https://www.vesselfinder.com/vessels/ANTIKITHIRA-IMO-9788980-MMSI-636020291 (accessed on 20 August 2022).
18. McGuire, J.J.; White, B. *Liquefied Gas Handling Principles on Ships and in Terminals*; Witherby & Co: London, UK, 2000.
19. Burckhardt Compression. LABY® Compressors. 2021. Available online: https://www.burckhardtcompression.com/solution/compressor-technologies/laby-compressor/ (accessed on 20 August 2022).
20. MYCOM Compressors. Available online: https://www.mayekawa.com/mycom/screw_compressors/ (accessed on 20 August 2022).

21. Morosuk, L. Cascade refrigeration machines with R744 as the working fluid for the high-temperature cascade. *Refrig. Eng. Technol.* **2016**, *52*, 12–17.
22. Lemmon, E.W.; Bell, I.H.; Huber, M.L.; McLinden, M.O. *Reference fluid Thermodynamic and Transport Properties Database (REFPROP), Version 10.0*; NIST Standard Reference Database 23; National Institute of Standards and Technology: Gaithersburg, MD, USA, 2018.